### Title
Rain, waves, and short-term evolution of composite seacliffs in southern California




### Journal
Marine Geology, 267(1-2)

### ISSN
00253227



### Authors
Young, Adam P
Guza, R.T.
Flick, R.E.
et al.



### Publication Date
2009-11-01

### DOI
10.1016/j.margeo.2009.08.008

# Rain, Waves, & Short-Term Evolution of Composite Seacliffs in Southern California

Adam P. Young[a,*], R.T. Guza[a], R.E. Flick[a], W.C. O'Reilly[a], and R. Gutierrez[b]

[a] Integrative Oceanography Division, Scripps Institution of Oceanography, University of California San Diego, 9500 Gilman Dr., La Jolla, CA, 92093-0209, USA

[b] Center for Space Research, The University of Texas at Austin, 3925 West Braker Lane, Suite 200, Austin, TX, 78759-5321, USA

* Corresponding author:
Email: adyoung@ucsd.edu,
Phone: +1-858-822-3378
Fax: +1-858-534-0300



A four-year time series of nine airborne LIDAR surveys were used to assess the roles of wave attack and rainfall on the erosion of 42 km of Southern California seacliffs. Nine continuous seacliff sections, separated by coastal lagoon mouths, all show maximum seacliff erosion in the rainiest time period (when wave energies were not particularly elevated), and in most sections the squared correlations between rainfall and erosion time series exceeded 0.8. Conversely, wave attack and cliff erosion were not statistically correlated in any section. Although rain and associated subaerial mechanisms such as groundwater seepage triggered most of the observed seacliff failures, wave attack accelerated seacliff erosion, with erosion rates of cliffs exposed to wave attack five times higher than at adjacent cliffs not exposed to waves. The results demonstrate the importance of both waves and rain in the erosion of Southern California seacliffs and suggest that the combined influences of marine and subaerial processes accelerate the erosion rate through positive feedbacks.

Keywords: coastal erosion; seacliff retreat; San Diego County; California



## 1. Introduction

Seacliffs comprise 80% of the world's coasts (Emery and Kuhn, 1982), where almost one quarter of the global population resides (Small and Nicholls, 2003). Seacliff erosion threatens coastal structures, public property, recreational resources, public safety, and major transportation corridors, notably along the California coast (Griggs *et al.*, 2005). To combat these problems, seawalls are increasingly used to prevent erosion. However, coarse grained seacliffs contribute sediment to beaches (Young and Ashford, 2006a), an important economic and cultural resource, and preventing seacliff erosion through armoring reduces the beach sand input. Effectively managing coastal areas will become increasingly challenging as coastal populations and sea levels continue to rise.

Seacliff erosion is broadly attributed to marine and subaerial (including subsurface) erosion mechanisms (Hampton and Griggs, 2004; Sunamura, 1992; Trenhaile, 1987). Subaerial mechanisms (*e.g.* groundwater processes, rilling, slope wash) act over the entire cliff face, and beneath the surface. Rainfall has been empirically linked to inland landsliding (Caine, 1980), where marine processes are not active, and serves as an indicator of subaerial forcing. In contrast, marine processes (*e.g.* wave-driven impact pressures and abrasion) act directly only at the cliff base, and only when tides and other water level fluctuations allow waves to reach the cliff. Therefore, the duration of wave attack is an indicator of marine forcing (Ruggiero *et al.*, 2001; Sallenger *et al.*, 2002). While marine and subaerial processes drive the erosion, geologic conditions dictate the resistance and control the seacliff failure mode.

Numerous studies have identified various marine, subaerial, and cliff-attribute related controls on the seacliff erosion process. For example cliff erosion has been related to wave action (Carter and Guy, 1998; Robinson, 1977; Ruggiero *et al.*, 2001; Wilcock *et al.*, 1998), groundwater (Hutchinson, 1969; Pierre and Lahousse, 2006), beach geometry (Dornbusch *et al.*, 2008; Jones and Williams, 1991; Sallenger *et al.*, 2002), cliff lithology (Benumof *et al.*, 2000; Collins and Sitar, 2008), cliff geometry (Edil and Vallejo, 1980; Emery and Kuhn, 1982), and tectonic activity (Komar and Shih, 1993). The identified controls are different in part due to observations of cliffs in different stages of development, and differences in local geology (Hampton and Griggs, 2004; Sunamura, 1992; Trenhaile, 1987). The importance ascribed to subaerial and marine processes also depends on sampling duration and frequency, and the wave and weather conditions during the observation period. For example large scale episodic events such as *El Niño* and earthquakes cause significant cliff erosion (Hapke and Richmond, 2002; Storlazzi and Griggs, 2000). This study builds upon this previous research to investigate the processes of short-term seacliff evolution in southern California using the unique data set made possible by regular, repeated LIDAR overflights.

Seacliff evolution has been conceptualized as a three-stage cycle (Everts, 1990; Hampton and Griggs, 2004; Sunamura, 1992; Trenhaile, 1987). In Stage 1, waves erode the cliff base, causing slope steepening and reducing cliff stability. Eventually, in Stage 2, a slope failure occurs, depositing talus material at the cliff base. The talus temporarily protects the cliff from direct wave action until the talus is removed during Stage 3, restoring direct wave attack, and completing the cycle (Figure 1). Stages 1 and 3 are dependent on marine processes and occur over longer time scales (Stage 1: years, Stage 3: weeks to years) than Stage 2, which often occurs abruptly and is frequently triggered by subaerial mechanisms (Bryan and Price, 1980; Edil and Vallejo, 1980; Hampton and Griggs, 2004; Hutchinson, 1969; May, 1971; McGreal, 1979; Pierre and Lahousse, 2006; Quigley and Di Nardo, 1980; Sunamura, 1992; Trenhaile, 1987). Stage 2 may occur in a series of cliff failures as instability propagates up the cliff face. Seawalls interrupt this natural cycle by preventing the wave action that reduces cliff stability at Stage 1, and removal of talus at stage 3.

Long-term seacliff morphology studies typically use historical topographic maps and aerial photographs to determine cliff top retreat (*e.g.* Benumof *et al.*, 2000; Dornbusch *et al.*, 2008; Pierre and Lahousse, 2006). Recent advances in Light Detection and Ranging

(LIDAR) now permit short-term, high-resolution monitoring and analysis of topographic changes in three dimensions. Previous seacliff studies utilizing LIDAR have investigated cliff changes between two surveys (Sallenger *et al.* 2002; Young and Ashford, 2006a, 2007, 2008), while others (Collins and Sitar, 2008; Rosser *et al.*, 2005) provide a time series of local cliff changes. Repeated, high-resolution and spatially extensive seacliff surveys are rare. This study builds upon the previous research by utilizing a unique regional four-year time series (May 2002 – March 2006) of nine airborne Light Detection and Ranging (LIDAR) surveys to quantify cliff erosion with change detection analysis and asses the roles of wave attack and rainfall on 42 km of southern California seacliffs. This detailed time-series of three dimensional cliff changes provides a unique, regional view of the processes that influence short-term seacliff erosion.



## 2. Study Area Description

### 2.1 Seacliffs

The seacliffs in our study area, ranging in height from 2-110 m, are generally composed of two geologic units: a lower unit of lithified Eocene and Miocene mudstone, shale, sandstone, and siltstone, and an upper unit of unlithified Pleistocene terrace deposits (Kennedy, 1975). Long-term cliff retreat rates range from 7 to 43 cm/yr (Benumof *et al.*, 2000; Everts, 1990; Hapke and Reid, 2007; Moore *et al.*, 1999). Geologic conditions (*e.g.* cliff resistance to erosion) can vary alongshore at a range of scales, contributing to variation of erosion rates. The studied cliffs are divided into nine continuous sections, based on general lithology and lagoon incisions (Figure 2).

Cliff retreat in the southern region (especially Solana Beach, Cardiff, and Leucadia) threatens extensive cliff top development, and has resulted in major seawall construction that reduces the cliff retreat rate (Young and Ashford, 2006b). Conversely, the cliff top in the northern region is relatively undeveloped and seawalls are absent. However, in the northern region, jetties interrupt natural littoral transport and contribute to formation of the broad beach fronting the Camp Pendleton seacliffs, preventing wave attack during the study period.



**2.2 Waves**

The seacliffs are exposed to waves generated by local winds and distant storms in both hemispheres. During winter, swell from the North Pacific and Gulf of Alaska are most energetic, whereas swell from the South Pacific dominates in summer. Waves reaching southern California cliffs undergo a complex transformation, and "shadows" of the Channel Islands create strong alongshore variations in wave height (Figure 2). The seasonal cycle (maximum wave energy in winter) is strongest in the southern sections. Historical data (Figure 3) indicates regional wave heights during the study period were typical.

**2.3 Rain**

San Diego's semi-arid Mediterranean climate is characterized by dry summers and occasionally wet winters, with 85% of rainfall occurring from November through March. Annual precipitation amounts vary from about 10-60 cm, and average 25 cm. Rainfall in the region tends to be episodic and several centimeters of rain often fall over a few days. The study period was relatively dry, except for the wet winter of 2004-2005 (Figure 3) when winter storms delivered about 56 cm of rain.



## 3. Methods

### 3.1 Topographic Change

Airborne LIDAR data was collected each spring and fall from May 2002 through March 2006 with an Optech Inc. Airborne Laser Terrain Mapper 1225 which made four passes at an altitude of 300-1000 m to provide a point density of approximately 3 points/$m^2$ on the cliff. A time series of topographic change for eight time intervals (Table 1), obtained by differencing successive digital elevation maps to create digital change grids (DCG), shows erosion (negative changes) at landslide source locations on the cliff face, and accretion (positive changes) at talus deposits at the cliff base (Figure 1). The net change (sum of positive and negative changes) is the material volume removed from the cliff face and base.

LIDAR data were processed into 0.5 $m^2$ resolution digital elevation models using the second of two LIDAR returns (the last return is the most representative of the ground surface) and a modified "natural neighbors" technique, which removes over-vertical features and maintains vertical cliff edges and complex topography. The large majority of these seacliffs lack the material strength required to maintain over-vertical features. However, localized areas of sea caves and notches can form at the base of cliffs in the southern region, notably in Solana Beach.

Time series of cliff change, and beach elevation at the cliff base, were estimated for 3-m long (in the alongshore direction) cliff compartments, well resolving changes in the alongshore geologic conditions. Major seawalls were identified using coastal maps and recent photographs (California Coastal Records Project, 2008; Flick, 1994) and assigned to the corresponding compartments.

*Errors*: Sources of errors in elevation change maps include the basic LIDAR observations, spatial interpolation, and vegetation. The vertical root mean square difference between two surveys ($RMS_Z$, Federal Geographic Data Committee, 1998), a measure of the total error, was estimated using three control sections; the San Onofre Nuclear Generating Station containment domes, a stabilized vegetated coastal slope in Cardiff, and a concrete-covered seacliff in Solana Beach. These three control sections represent the range of slopes and vegetative conditions of the seacliffs within the study area. The average $RMS_Z$ of all control sections and intervals was 19 cm, with standard deviation of 3 cm.

*Digital Change Grid Filtering*: The digital change grids were filtered and edited to remove noise and erroneous data. First, all grid cells with a vertical change of less than 38 cm (twice the $RMS_Z$ error) were neglected. Next, a minimum topographic footprint was imposed, requiring at least 10 connected cells of positive or negative change, thus enforcing a minimum change area of 2.5 $m^2$. This filtering identifies individual landslides and talus deposits with a minimum volume of about 1 $m^3$ (if all 10 cells had 38 cm of change). In practice, the minimum volume was approximately 2 $m^3$. Finally, the filtered DCG data were edited visually to remove spurious changes caused by construction or vegetation.

*Data Limitations*: The calculated change volumes underestimate the actual erosion because only relatively large volume (> 2 $m^3$) and large footprint (> 2.5 $m^2$) slides are detected. The neglected small events may play an important role in short-term seacliff evolution (Rosser *et al.*, 2005; Young and Ashford, 2007), and their volume contribution for the study period is unknown. However, based on previous research for a small portion of the study area (Young and Ashford, 2007), the volume contribution of these small events are estimated at approximately 15-30% of the total eroded volume that occurred.

If positive and negative volumes have significantly different void fractions, these change volumes are not directly comparable. For example, the volume eroded from the cliff face will be smaller than the associated talus deposit if the talus is less dense owing to larger voids. However, the void fractions are unknown.

### 3.2 Waves and Runup

The wave impact duration (WID) is defined as the number of hours the total water level was above the beach elevation at the cliff base. Hourly time series of beach elevation at the cliff base were computed for each compartment by linearly interpolating the elevation between each survey. The total water level (Figure 4) is the sum of tides and the vertical height of wave runup (Collins and Sitar, 2008; Kirk *et al.*, 2000; Ruggiero *et al.*, 2001; Shih *et al.*, 1994). Tidal fluctuations are more than 2m during spring tides, so large swells arriving during relatively low tide may not even reach the cliffs, whereas moderate swell arriving during high tide can have significant impact duration. Hourly water levels seaward of the surfzone, including tides, atmospheric pressure and wind effects, were obtained from the La Jolla tide gauge #94101230 (http://tidesandcurrents.noaa.gov), located in about 7m water depth at the southern end of the study area.

A wave buoy network (CDIP, http://cdip.ucsd.edu) was used to estimate hourly wave conditions at "virtual buoys" located in 10-m depth, seaward of each cliff section (Figure 2). The effects of complex bathymetry in the Southern California Bight, and of varying beach orientation and wave exposure, were simulated at the virtual buoy locations with a spectral refraction wave model initialized with offshore buoy data (O'Reilly and Guza, 1991; O'Reilly and Guza, 1998). The vertical height of wave runup was approximated as $R_{2\%}$, the level exceeded by 2% of wave uprushes

$$R_{2\%} = 1.1\left\{0.35\beta_f\left(H_oL_o\right)^{0.5} + \left(\left[H_oL_o\left(0.563\beta_f^2 + 0.004\right)\right]^{0.5}\right)/2\right\} \qquad (1)$$

where $H_o$ and $L_o$ characterize the incident wave height and wavelength (Stockdon *et al.*, 2006). The beach slope ($\beta_f$) was estimated from the LIDAR data as the median upper beach slope (a 20m swath centered on the mean high water contour) of each compartment. Time series of hourly total water level (tide gage plus $R_{2\%}$) and sand level at the cliff base were used to estimate wave impact duration (WID, number of hours the total water level exceeded the sand level during the time interval).

**3.3 Rain**

Rainfall parameters including intensity, duration, antecedent rainfall, and cumulative total have been used to assess subaerial influences (Aleotti, 2004; Caine, 1980; Campbell, 1974; Collins and Sitar, 2008; Glade *et al.*, 2000; Hutchinson, 1969; Lahousse and Pierre, 2006). In the present observations, the timing of erosion within a survey period is unknown, the cliff response to individual storms cannot be assessed, and the applicability of the various parameterizations cannot be tested. Below we show that a simple rainfall metric, cumulative total rainfall during each time interval, is correlated with the cumulative total erosion in that interval. Cumulative rainfall totals in each observation interval were evaluated from daily rainfall data at San Diego's Lindbergh Field (www.wrh.noaa.gov).

**4. Results**

### 4.1 Rainfall and Erosion Correlation

In all sections, the maximum erosion volume occurred during the wettest period (winter of 2004-2005), and in eight of nine cliff sections erosion volumes correlated well with rainfall ($r^2$ between 0.66-0.95, Table 2). The correlation at San Onofre is low ($r^2$=0.2) because a deep-seated landslide, reactivated in the wet winter of 2004-2005, continued to move for the remainder of the study period. This effectively provided a continuous failure with high erosion rates during times of little rainfall (Figure 5B). In all sections except the anomalous San Onofre section, the second largest amount of erosion occurred in the second rainiest interval (winter 2002-2003). Region-wide cliff erosion occurred during rainy periods, and in these observations rainfall and wave attack were not correlated. The triggering role of rain was therefore more easily isolated than in time periods when waves and rain are correlated (possibly during an *El Niño*).



### 4.2 Wave and Erosion Correlation

Wave action is a fundamental part of the erosion cycle, and without wave action, the cliff erosion rate and cliff slope decrease with time to the lower values characteristic of weathered inland cliffs (Bucknam and Anderson, 1979). This point is illustrated by comparing the adjacent cliff sections in Camp Pendleton North and San Onofre, which have similar compositions and height. In Camp Pendleton North, where waves did not reach the cliff base, the net erosion rate was 1.0 $m^3$/m-yr compared with 4.9 $m^3$/m-yr for the San Onofre cliffs, which were impacted by waves.

Although waves accelerate cliff erosion, waves and erosion were not significantly correlated in any section ($r^2$ <0.2, *i.e.*, not significant at the 80% level). Multiple regressions using both waves and rain versus erosion yield correlations only slightly higher than those with rain alone. Wave-erosion correlations are low because volumes eroded in Stage 1 are trivial compared to the amounts in Stages 2 and 3. Additionally, the lag time between Stage 1 (wave action) and Stage 2 (cliff failure) probably also prevented higher correlations between wave action and erosion. The lag-time is unknown and could not be established with this data set.

**4.3 Sub-Sections**

Variable-length subsections were used to identify areas where erosion was significantly correlated with waves (WID & Erosion, Figure 6). These cliffs, scattered throughout the region, were predominately in Stage 3, and comprised about 10% of the study area length and 20% of the eroded volume. In this study, the majority of the resolved erosion occurred in Stage 2, thus leading to high correlations between rainfall and erosion. Had talus erosion been measured much more frequently, such as daily, rather than every six months, the erosion data might be better correlated with wave impact. Similarly, waves and erosion might be correlated at time scales longer than the four years of the present study.

Wave impact durations and net erosion rates (Figure 6A and 6E), are both highly variable alongshore, but these spatial variations are uncorrelated. The variation in wave impact duration is caused by alongshore variations in the wave field and, more importantly, variations in the back-beach elevation. For example, the back-beach elevations in Solana Beach are relatively low, and high tide alone (without waves) can reach the cliffs. The spatial variation in net erosion associated with variable wave impact is masked by alongshore variability in geologic conditions (*e.g.* cliff erodability and cliff height) and seawalls, which implies that the cliff resistance to erosion is an important factor.

**4.4 Deep-Seated Landslides**

Deep-seated landslides at San Onofre accounted for a significant amount of eroded material (Figure 5B, zone of highest erosion in Figure 6E). At least one major relic landslide was reactivated by heavy rainfall. This area experienced net erosion rates more than twenty times the regional average. After initial movement, wave action presumably removed material at the slide toe, reducing lateral resistance and causing further slide movement [*Hutchinson*, 1969]. This sequence departs from the general stages of cliff evolution described above. With deep-seated landslides, cliff failure and talus removal (Stages 2 and 3) occur concurrently and semi-continuously, and Stage 1 (basal erosion of *in situ* cliff material) may be absent.

**5. Discussion and Summary**

All nine cliff sections show maximum seacliff erosion in the rainiest time period, when wave energies were not particularly elevated. In eight of the nine sections, squared correlations between rainfall and erosion were significant, and often >0.8. Rain is clearly the critical triggering mechanism for most of the significant cliff failures in these observations and the timing of heavy rainfall may assist in predicting cliff failures. Our results show that subaerial processes are important in the short-term evolution of the southern California seacliffs, which is consistent with numerous previous cliff studies in other regions of the world.

However, marine and subaerial erosion processes are inter-dependent, owing to the feedback mechanisms in the cliff erosion cycle. For triggering mechanisms to instigate a cliff failure, wave action must first create unstable slopes. Therefore, the rate of rain-triggered cliff failures depends on both waves and rain. Thus, although rain triggered most of the observed seacliff failures, wave attack accelerated seacliff erosion, with rates in areas exposed to wave attack five times higher than in adjacent areas not exposed to wave attack. Similarly, we suggest that the observed erosion rates with waves and rain would be reduced without rain, because the rain-triggered slides would likely be replaced by fewer, wave-triggered slides. In addition, as rain triggers more frequent landslides, new cliff material becomes more rapidly exposed and subject to deterioration through weathering and fatigue, thus weakening the cliff materials. In turn, this allows wave action to erode the deteriorated cliff material more effectively. The results show the importance of both marine and subaerial processes to seacliff erosion, and suggest that rain and waves combine to produce much higher erosion rates than would occur with either process alone. These conclusions are limited by the relatively short (four-year) duration of the observations. Additional temporally and spatially well-resolved cliff observations, extending over decades, are needed.

**Acknowledgments**

LIDAR surveys were sponsored by the U.S. Army Corps of Engineers as part of the Southern California Beach Processes Study. Wave data was provided by the Coastal Data Information Program (CDIP), funded by the California Department of Boating and Waterways, and the U.S. Army Corps of Engineers. APY received Post-Doctoral Scholar support from the California Department of Boating and Waterways Oceanography Program.

**Figures**

Figure 1. Changes in cliff elevation (colors) superimposed on aerial photographs in Solana Beach, CA. (Top) Stage 2 cliff failure (red) and talus deposit (blue). (Bottom) Subsequent time interval at the same location showing the removal of the talus deposit by wave action (Stage 3) and a new Stage 2 cliff failure about 150m to the north. The associated cliff change volumes are 1: -260 $m^3$, 2: 185 $m^3$, 3: -95 $m^3$, 4: 5 $m^3$, 5: -360 $m^3$, 6: -285 $m^3$, 7: 115 $m^3$.



Figure 2. (Top) Setting of the sea cliffs and typical distribution of significant wave heights from winter northwesterly swell (March 10, 2005, 285°, 17 second period). The islands create wave shadows and alongshore variation of nearshore wave height. (Bottom) The nine seacliff sections and locations of the corresponding virtual buoys.

Figure 3. Historical average monthly significant wave height (upper) in the Southern California Bight (Santa Monica Buoy 46025, www.ndbc.noaa.gov) and rainfall (lower) in San Diego, CA (www.wrh.noaa.gov). Sampling intervals during the study period are indicated.

Figure 4. Schematic of waves impacting a cliff. Wave impact occurs when the tide plus vertical runup exceeds the sand elevation at the cliff base. Virtual buoys used to calculate runup are located seaward of each cliff section in 10 m water depth (Figure 2).

Figure 5. Normalized ($X_i / X_{max}$) total erosion, rainfall, and wave impact duration versus time for (A) all regions except San Onofre. The squared correlation between erosion and rainfall is high ($r^2$ =0.93), and between erosion and wave impact duration is low ($r^2$=0.05). (B) San Onofre, where rainfall and erosion are correlated through time interval 6 ($r^2$ =0.87), when rainfall reactivated a large deep-seated landslide and continuing erosion.

Figure 6. (A) Alongshore and temporal variation of wave impact duration (number of potential hours waves reached the cliff base, log scale), (B) temporal variation of rainfall, (C) alongshore and temporal variation of cliff erosion (log scale) and, (D) sub-sectional alongshore variation of temporal correlations ($r^2$) of erosion & wave impact duration and erosion & rainfall. The sub-section lengths are variable and are delineated by locations where wave impact duration & erosion were significantly correlated. Note the strong relationship between seacliff erosion and rainfall. (E) Alongshore net erosion rate (90 m moving average, log scale).

**References**

Aleotti, P., 2004. A warning system for rainfall-induced shallow failures. *Engr. Geol. 73*, 247-265.

Benumof, B., Storlazzi, C., Seymour, R., Griggs, G., 2000. The relationship between incident wave energy and seacliff erosion rates: San Diego County, California. *J. Coastal Res. 16*. 1167- 1178.

Bryan, R. B., Price, A. G. 1980. Recession of the Scarborough Bluffs, Ontario, Canada. *Zeitschrift fur Geomorphologie, Supplement-Band 34*, 48–62.

Bucknam, R. C., Anderson, R. E., 1979. Estimation of fault-scarp ages from a scarp-height-slope-angle relationship. *Geology 7*. 11-14.

Caine, N., 1980. The rainfall intensity duration control of shallow landslides and debris flows. *Geogr. Ann. A 62*. 23–27.

California Coastal Records Project, 2008. www.californiacoastline.org.

Campbell, R. H., 1974. Debris flow originating from soil slips during rainstorms in southern California. *Q. J. Engng. Geol. 7*, 339-349.

Carter, C. H., Guy, D. E.,1988. Coastal erosion: processes, timing and magnitude at the bluff toe. *Mar. Geol. 84*. 1–17.

Collins, B. D., Sitar, N., 2008. Processes of coastal bluff erosion in weakly lithified sands, Pacifica, California, USA. *Geomorphology 97*. 483-501.

Dornbusch, U., Robinson, D. A., Moses, C. A., Williams, R. B. G., 2008. Temporal and spatial variations of chalk cliff retreat in East Sussex, 1873 to 2001. *Mar. Geol. 249*. 271-282.

Edil, T. B., Vallejo, L. E.,1980. Mechanics of coastal landslides and the influence of slope parameters. *Eng. Geol.16*. 83–96.

Emery, K. O., Kuhn, G. G., 1982. Sea cliffs: their processes, profiles, and classification. *Geol. Soc. Am. Bull. 93*. 644-654.

Everts, C. H., 1990. Sediment budget report Oceanside Littoral Cell, Coast of California Storm and Tidal Wave Study 90-2, U.S. Army Corp of Engineers, Los Angeles District, 110 pp.

Federal Geographic Data Committee, 1998. Geospatial positioning accuracy standards, FGDC-STD-007.3-1998, 28 pp.

Flick, R. E., 1994. *Shoreline Erosion Assessment and Atlas of the San Diego Region*, 2 volumes. Sacramento, California: California Department of Boating and Waterways.

Glade, T., Crozier, M., Smith, P., 2000. Applying probability determination to refine landslide-triggering rainfall thresholds using empirical "antecedent daily rainfall model." *Pure Appl. Geophys. 157*, 1059-1079.

Griggs, G., Patsch, K., Savoy, L., 2005. *Living with the Changing California Coast*, University of California Press, Berkeley, California, 540 pp.

Hampton, M. A., Griggs, G. B. (eds.), 2004. Formation, Evolution, and Stability of Coastal Cliffs – Status and Trends. USGS Professional Paper 1683, 123 pp.

Hapke C., Richmond, B., 2002. The impact of climatic and seismic events on the short-term evolution of seacliffs based on 3-D mapping, northern Monterey Bay, California, *Mar. Geol. 187*. 259- 278.

Hapke, C. J., Reid, D., 2007. National Assessment of Shoreline Change, Part 4: Historical Coastal Cliff Retreat along the California Coast: U.S. Geological Survey Open-file Report 2007-1133.

Hutchinson, J. N., 1969. A reconsideration of the coastal landslides at Folkestone Warren, Kent. *Géotechnique 19*. 6-38.

Jones, D. G., Williams, A. T., 1991. Statistical analysis of factors influencing coastal erosion along a section of the west Wales coast, UK. *Earth Surf. Proc. Land. 23*. 1123-1134.

Kennedy, M. P., 1975. Geology of the San Diego metropolitan area, western area. California Division of Mines and Geology Bulletin 200, 56 pp.

Kirk, R. M., Komar, P. D., Allen, J. C., Stephenson, W. J., 2000. Shoreline erosion on Lake Hawea, New Zealand, caused by high lake levels and storm-wave runup. *J. Coastal Res. 16*. 346-356.

Komar, P. D., Shih S. M., 1993. Cliff erosion along the Oregon coast; a tectonic sea level imprint plus local controls by beach processes. *J. Coastal Res. 9*. 747–765.

May, V. J., 1971. The retreat of chalk cliffs. *The Geographical Journal 137*, 203-206.

McGreal, W. S. 1979. Factors promoting coastal slope instability in southeast County Down, N. Ireland. *Zeitschrift für Geomorphologie 23*, 76-90.

Moore, L. J., Benumof, B. T., Griggs, G. B., 1999. Coastal erosion hazards in Santa Cruz and San Diego Counties, California. In: Crowell, M. and Leatherman, S.P. (eds.), Coastal Erosion Mapping and Management. *J. Coastal Res. SI 28*. 121-139.

O'Reilly, W. C., Guza, R. T., 1991. Comparison of spectral refraction and refraction-diffraction wave models. *J. Waterway Port C-ASCE 117*. 199-2l5.

O'Reilly, W. C., Guza, R. T., 1998. Assimilating Coastal Wave Observations in Regional Swell Predictions. Part I: Inverse Methods. *J. Phys. Oceanogr. 28*. 679–691.

Pierre, G., Lahousse, P., 2006. The role of groundwater in cliff instability: an example at Cape Blanc-Nez (Pas-de-Calais, France). *Earth Surf. Proc. Land. 31*. 31-45.

Robinson, L. A., 1977. Marine erosive processes at the cliff foot. *Mar. Geol. 23*. 257–271.

Quigley R. M., Di Nardo L. R. 1980. Cyclic instability modes of eroding clay bluffs, Lake Erie, Northshore bluffs at Port Bruce, Ontario, Canada. *Zeitschrift für Geomorphologie. Suppl. Bd 34*, 39–47.

Rosser, N. J., Petley, D. N., Lim, M., Dunning, S. A., Allison, R. J., 2005. Terrestrial laser scanning for monitoring the process of hard rock coastal cliff erosion. *Q. J. Eng. Hydroge. 38*. 363–375.

Ruggiero, P., Komar, P. D., McDougal, W. G., Marra, J. J., Beach, R. A., 2001. Wave Runup, Extreme Water Levels and the Erosion of Properties Backing Beaches. *J. Coastal Res. 17*. 407-419.

Sallenger Jr., A. H., Krabill, W., Brock, J., Swift, R., Manizade, S., Stockdon, H., 2002. Sea-cliff erosion as a function of beach changes and extreme wave runup during the 1997–1998 El Niño. *Mar. Geol. 187*. 279–297.

Shih, S. M., Komar, P. D., Tillotson, K. J., McDougal, W. G., Ruggiero P., 1994. Wave run-up and sea-cliff erosion. In Coastal Engineering 1994 Proceedings, 24th International Conference, American Society of Civil Engineers, 2170–2184.

Small, C., Nicholls, R. J., 2003. A global analysis of human settlement in coastal zones. *J. Coastal Res. 19*. 584-599.

Stockdon, H. F., Holman, R. A., Howd, P. A., Sallenger Jr., A. H., 2006. Empirical parameterization of setup, swash, and runup. *Coast. Eng. 53*. 573-588.

Storlazzi, C. D., Griggs, G. B., 2000. Influence of El Niño-Southern Oscillation (ENSO) events on the evolution of central California's shoreline. *Geol. Soc. Am. Bull. 112*. 236–249.

Sunamura, T., 1992. *Geomorphology of Rocky Coasts*, John Wiley and Sons, New York, 302 pp.

Trenhaile, A. S., 1987. *The Geomorphology of Rock Coasts*, Oxford University Press, New York, 384 pp.

Wilcock, P. R., Miller, D. S., Shea, R. H., Kerkin, R. T., 1998. Frequency of effective wave activity and the recession of coastal bluffs: Calvert Cliffs, Maryland. *J. Coastal Res. 14*. 256–268.

Young, A. P., Ashford, S. A., 2006a. Application of airborne LIDAR for seacliff volumetric change and beach sediment contributions. *J. Coastal Res. 22*. 307-318.

Young, A. P., Ashford, S.A., 2006b. Performance evaluation of seacliff erosion control methods. *Shore & Beach 74*. 16-24.

Young, A. P., Ashford, S. A., 2007. Quantifying sub-regional seacliff erosion using mobile terrestrial LIDAR. *Shore & Beach 75*. 38-43.

Young, A. P. and Ashford, S. A., 2008. Instability investigation of cantilevered seacliffs. *Earth Surface Processes and Landforms 33*, 1661-1677.


Figure 1
Stage 2
Stage 3
Stage 2
1
2
3
4
5
6
7
Surficial Erosion
+ 5m Vertical Change - 5m
0 25 50 Meters
N

Figure 2

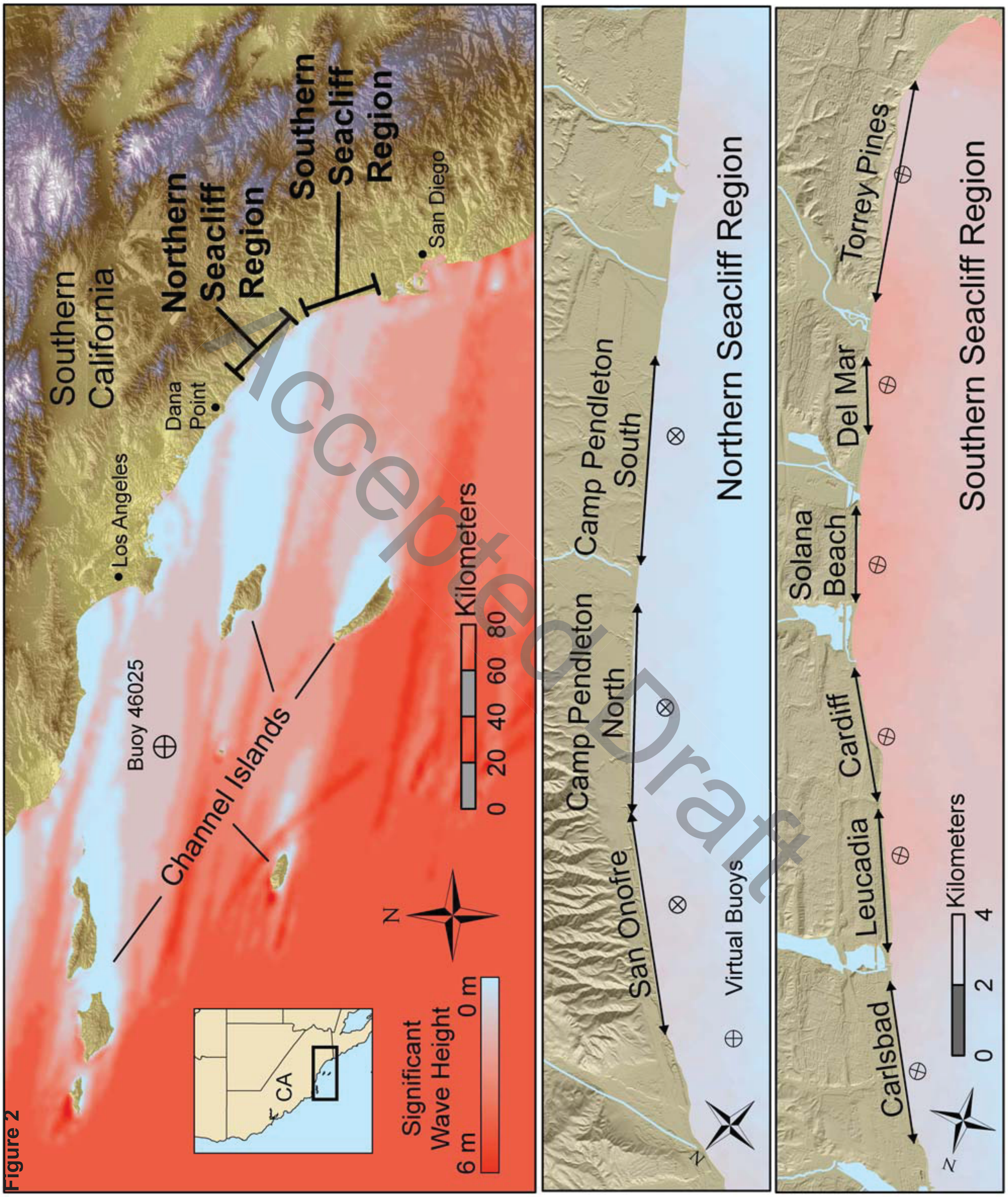
Southern California
Northern Seacliff Region
Southern Seacliff Region
San Diego
Dana Point
Los Angeles
Buoy 46025
Channel Islands
Kilometers
0 20 40 60 80
N
CA
Significant Wave Height
6 m
0 m
San Onofre
Camp Pendleton North
Camp Pendleton South
Virtual Buoys
Northern Seacliff Region
Carlsbad
Leucadia
Cardiff
Solana Beach
Del Mar
Torrey Pines
Southern Seacliff Region
Kilometers
0 2 4

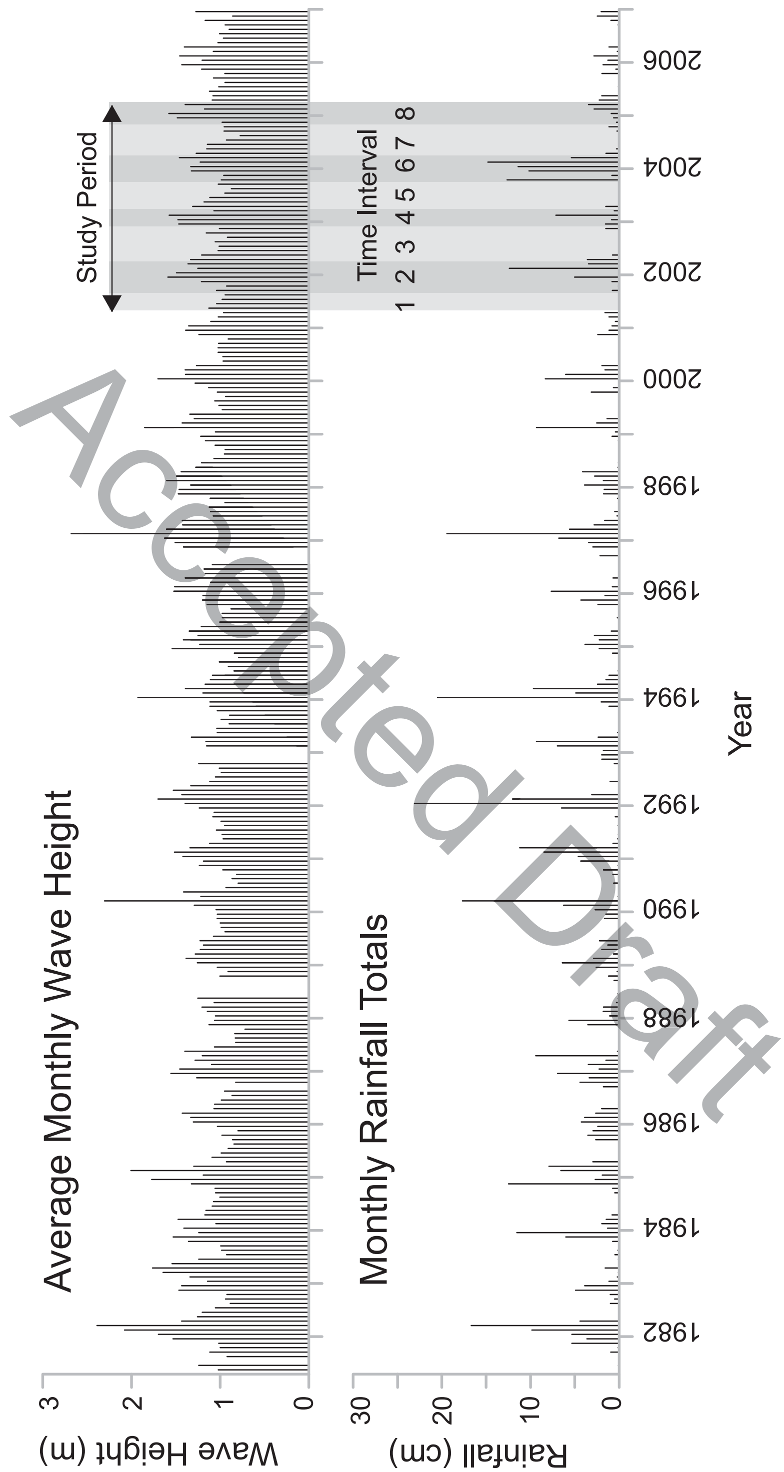
Average Monthly Wave Height
Wave Height (m)
0
1
2
3
Monthly Rainfall Totals
Rainfall (cm)
0
10
20
30
Study Period
Time Interval
1 2 3 4 5 6 7 8
1982
1984
1986
1988
1990
1992
1994
1996
1998
2000
2002
2004
2006
Year

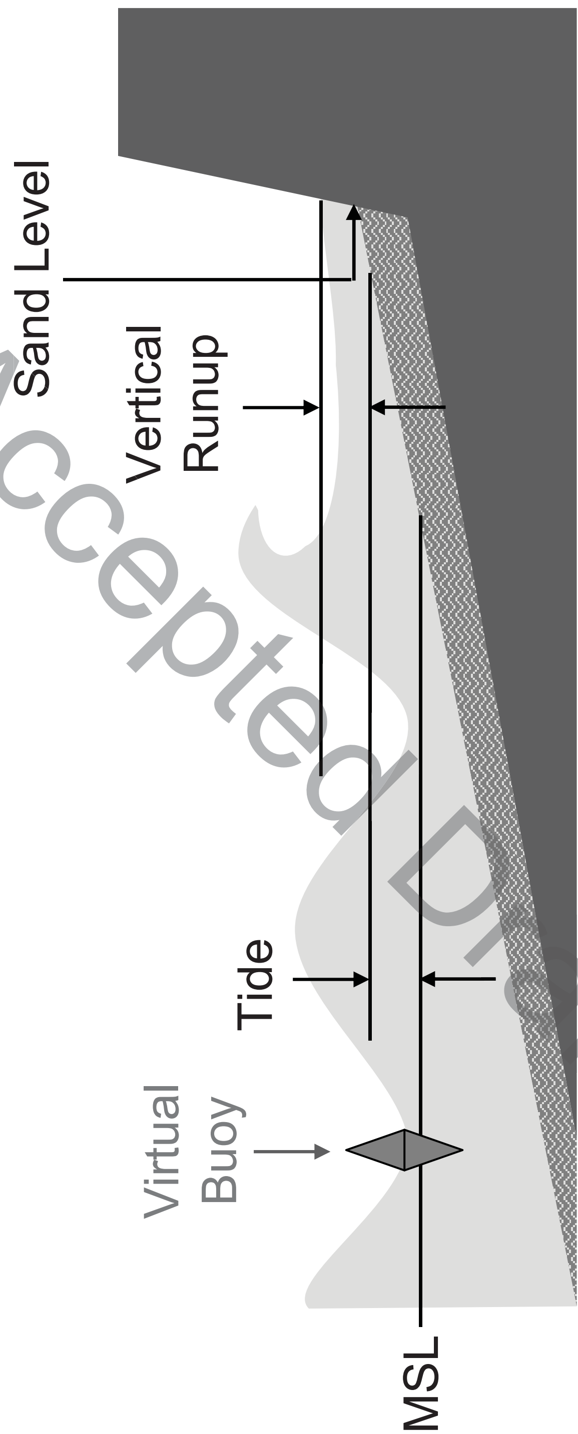
Sand Level
Vertical
Runup
Tide
Virtual
Buoy
MSL

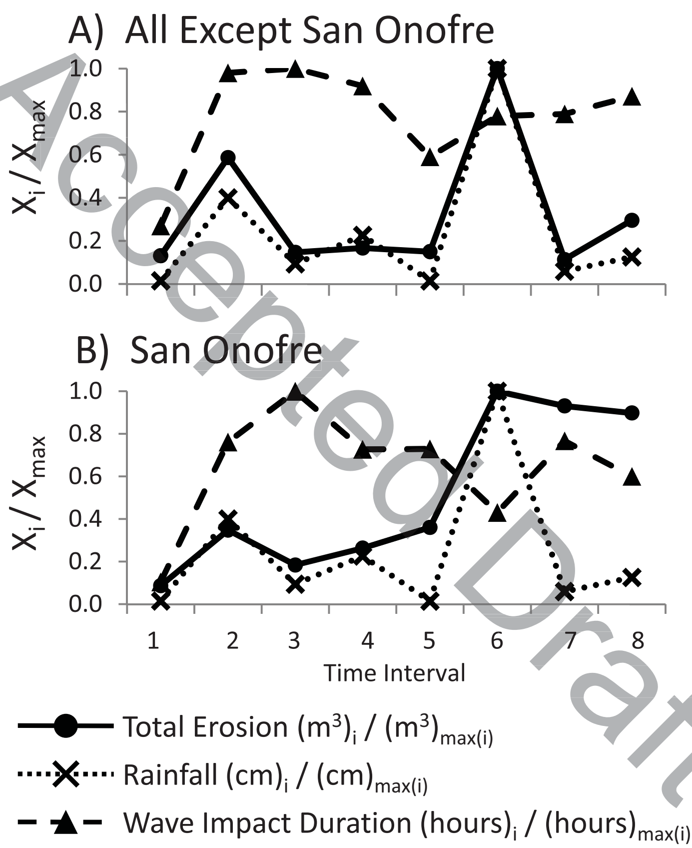
A) All Except San Onofre
1.0
0.8
0.6
0.4
0.2
0.0
Xi / Xmax
B) San Onofre
1.0
0.8
0.6
0.4
0.2
0.0
Xi / Xmax
1
2
3
4
5
6
7
8
Time Interval
Total Erosion (m3)i / (m3)max(i)
Rainfall (cm)i / (cm)max(i)
Wave Impact Duration (hours)i / (hours)max(i)

**Figure 6**

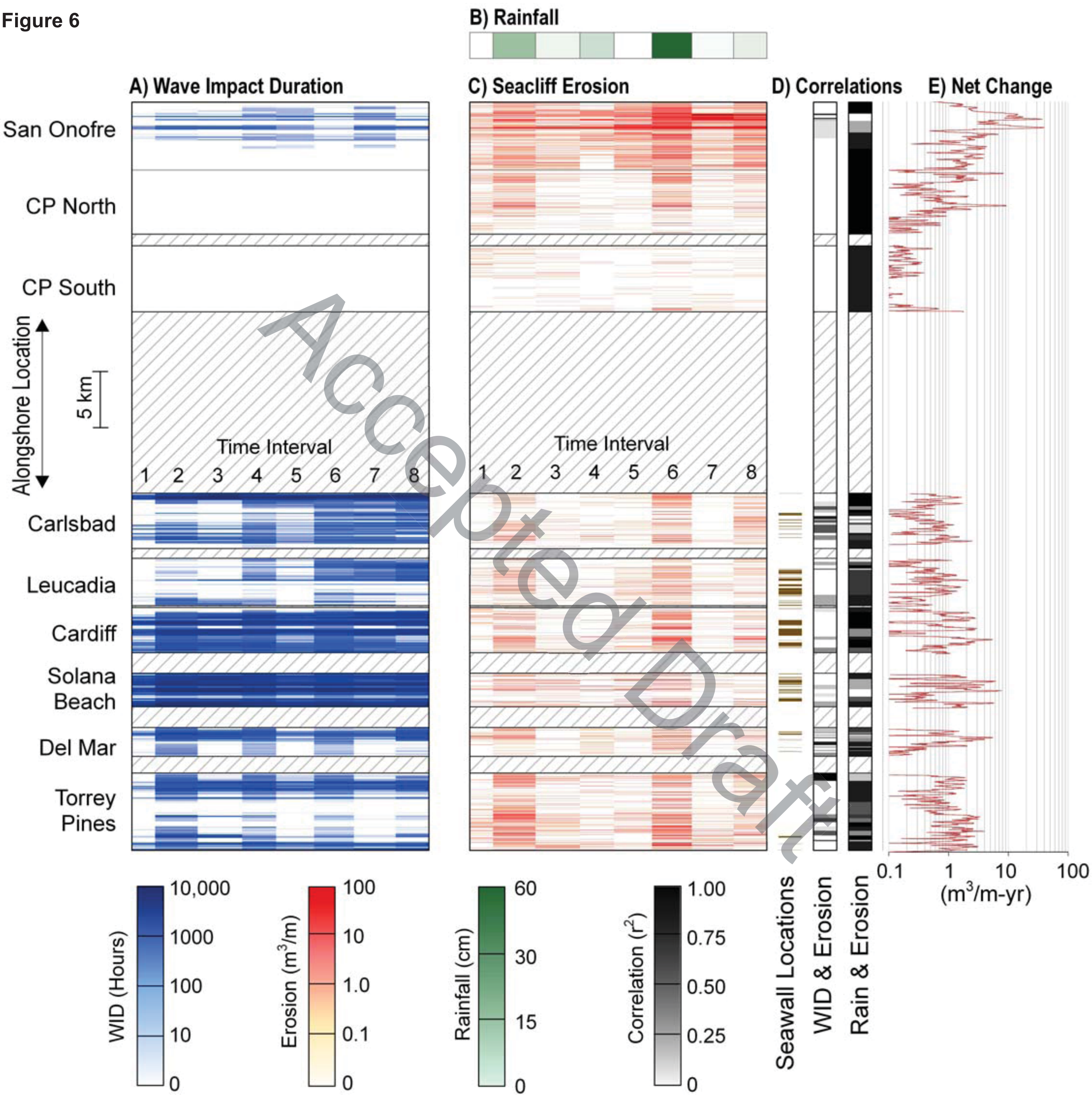
B) Rainfall
A) Wave Impact Duration
C) Seacliff Erosion
D) Correlations
E) Net Change
San Onofre
CP North
CP South
Alongshore Location
5 km
Time Interval
1 2 3 4 5 6 7 8
Carlsbad
Leucadia
Cardiff
Solana Beach
Del Mar
Torrey Pines
0.1 1 10 100
(m³/m-yr)
WID (Hours)
10,000
1000
100
10
0
Erosion (m³/m)
100
10
1.0
0.1
0
Rainfall (cm)
60
30
15
0
Correlation (r²)
1.00
0.75
0.50
0.25
0
Seawall Locations
WID & Erosion
Rain & Erosion

**Table 1**


**Table 1. Interval Information**

| Interval | Start Date | Season | Number of Days | Precipitation (cm) | Negative Change ($m^3$) | Positive Change ($m^3$) | Net Change ($m^3$) |
|---|---|---|---|---|---|---|---|
| **1** | 5/22/2002 | Summer | 110 | 0.8 | 10,400 | 1,300 | 9,100 |
| **2** | 9/9/2002 | Winter | 200 | 21.9 | 45,100 | 4,100 | 41,000 |
| **3** | 3/28/2003 | Summer | 210 | 5.1 | 14,800 | 2,300 | 12,500 |
| **4** | 10/24/2003 | Winter | 161 | 12.4 | 18,800 | 2,900 | 15,900 |
| **5** | 4/2/2004 | Summer | 179 | 0.8 | 21,400 | 2,700 | 18,700 |
| **6** | 9/28/2004 | Winter | 188 | 54.8 | 91,600 | 22,200 | 69,400 |
| **7** | 4/4/2005 | Summer | 197 | 3.3 | 40,100 | 23,300 | 16,800 |
| **8** | 10/18/2005 | Winter | 157 | 6.9 | 48,900 | 9,800 | 39,100 |
| Total | | | 1402 | 105.8 | 291,100 | 68,600 | 222,500 |

**Table 2. Section Information, Correlations ($r^2$), and Confidence Levels (CL%)**

| | Section Length (km) | Average Cliff Height (m) | Average Net Change ($m^3$/m-yr) | Percent Length of Seawalls (%) | Correlation Rainfall & Erosion ($r^2$) | (CL %) |
|---|---|---|---|---|---|---|
| San Onofre | 5.8 | 38 | 4.9 | 0 | 0.22 | 76 |
| CP North | 5.5 | 27 | 1.0 | 0 | 0.95 | 99 |
| CP South | 5.7 | 13 | 0.2 | 0 | 0.83 | 99 |
| Carlsbad | 4.8 | 16 | 0.5 | 10 | 0.78 | 99 |
| Leucadia | 4.1 | 24 | 0.5 | 37 | 0.76 | 99 |
| Cardiff | 3.9 | 23 | 1.1 | 38 | 0.89 | 99 |
| Solana Beach | 2.9 | 24 | 1.5 | 35 | 0.66 | 98 |
| Del Mar | 2.5 | 18 | 0.9 | 11 | 0.87 | 99 |
| Torrey Pines | 6.6 | 70 | 1.2 | 3 | 0.90 | 99 |
| All | 41.7 | 31 | 1.4 | 12 | 0.76 | 99 |